Non-Born−Oppenheimer Molecular Dynamics

AHREN W. JASPER, SHIKHA NANGIA, CHAOYUAN ZHU, AND DONALD G. TRUHLAR*

Department of Chemistry and Supercomputing Institute, University of Minnesota, 207 Pleasant Street SE, Minneapolis, Minnesota 55455-0431

Received April 4, 2005

ABSTRACT

Electronically nonadiabatic or non-Born−Oppenheimer (non-BO) chemical processes (photodissociation, charge-transfer, etc.) involve a nonradiative change in the electronic state of the system. Molecular dynamics simulations typically treat nuclei as moving classically on a single adiabatic potential energy surface, and these techniques are not immediately generalizable to non-BO systems due to the inherently quantum mechanical nature of electronic transitions. Here we generalize the concept of a single-surface molecular dynamics trajectory to that of a coupled-surface non-BO trajectory that evolves "semiclassically" under the influence of two or more electronic states and their couplings. Five non-BO trajectory methods are discussed. Next, we summarize the results of a series of systematic studies using a database of accurate quantum mechanical reaction probabilities and internal energy distributions for several six-dimensional model bimolecular scattering collisions. The test set includes three kinds of prototypical nonadiabatic interactions: conical intersections, avoided crossings, and regions of weak coupling. We show that the coherent switching with decay of mixing (CSDM) non-BO trajectory method provides a robust and accurate way to extend molecular dynamics to treat electronically nonadiabatic chemistry for all three kinds of nonadiabatic interactions, and we recommend it for molecular dynamics simulations involving nonradiative electronic state changes.

1. Introduction

Chemical processes involve both nuclear motions (such as molecular vibrations and rotations) and electronic motions (charge transfer, internal conversion, etc.). Chemical dynamics simulations may be simplified by making a Born−Oppenheimer (BO) separation of the nuclear and electronic motions, where the electrons are assumed to respond instantaneously (adiabatically) to changes in the nuclear coordinates, and the resulting nuclear motion evolves under the influence of a single adiabatic potential energy surface or, equivalently, is governed by the gradient of this surface, which is the force field. The BO separation is useful computationally because (1) it allows the nuclear and electronic problems, which usually correspond to very different time scales, to be solved independently and (2) separate kinds of theory may be used to treat the nuclear and electronic motions.

For many systems, nuclear motion is often well described by using classical mechanics. Classical simulations are often called trajectory calculations or "molecular dynamics".[1] Molecular dynamics has proven itself to be a useful tool for many areas of chemistry from drug design to materials science. Classical simulations neglect quantum effects, such as nuclear tunneling and electronic transitions, and therefore molecular dynamics may not be accurate (or even applicable) for systems where such effects play an important role.

In this Account, we discuss recent progress in incorporating nonradiative electronic transitions into classical simulations, thus extending molecular dynamics to new kinds of reactions, including visible and ultraviolet photochemistry, collisions of electronically excited species, chemiluminescence, and many recombination reactions, heterolytic dissociations, and electron transfer processes. These processes may be called non-BO processes or electronically nonadiabatic processes because they involve a breakdown of the BO separation. In such processes, the nuclear and electronic motions are coupled, that is, nuclear motions cause a change in the electronic state and electronic state changes affect the overall nuclear motion.

Section 3 describes the generalization of the concept of a BO molecular dynamics trajectory on a single potential energy surface to a non-BO trajectory.[2−17] The dynamics of a non-BO trajectory depends on two or more potential energy surfaces and their couplings, as well as on a set of electronic variables, which describe the overall electronic state of the system, as discussed in section 2.

2. Representations

For non-BO systems, where two or more electronic states (α, β, ...; $\beta \neq \alpha$) are coupled via BO breakdown terms, a potential energy surface may be associated with each electronic state.[14,18−24] The specific form of these surfaces depends on how one chooses to represent the electronic wave function. In the adiabatic representation, the electronic eigenvectors diagonalize the electronic Hamiltonian matrix at fixed nuclear coordinates. Then the lowest-energy surface corresponds to the usual BO ground-state

Ahren W. Jasper was born in Minneapolis in 1976. He received a B.A. from Gustavus Adolphus College in 1998 and a Ph.D. from the University of Minnesota in 2003, where his advisor was Donald Truhlar. He is currently an MSI Research Scholar at the University of Minnesota.

Shikha Nangia was born in New Delhi, India, in 1976. She received a B.Sc. (Honors) at University of Delhi in 1998 and an M.Sc. at Indian Institute of Technology (IIT) in Delhi in 2000. Presently, she is working on her doctoral research with Donald Truhlar at the University of Minnesota in the field of nonadiabatic dynamics, direct calculation of multistate diabatic potential energy surfaces, and fitting coupled potential energy surfaces for nonadiabatic processes.

Chaoyuan Zhu was born in Hailar, China, in 1956. He received B.A. and M.S. degrees from Sichuan University, and a Ph.D. in Theoretical Nuclear Physics from Academica Sinica in Shanghai in 1990. He received a second Ph.D. in Chemical Physics in 1993 from the Institute for Molecular Science in Okazaki, Japan, where his adviser was Hiroki Nakamura. In 1993, he joined the Theoretical Division of the Institute for Molecular Science as an assistant professor. In 2002, he became a research associate at the University of Minnesota.

Donald G. Truhlar was born in Chicago in 1944. In 1965, he received a B.A. from St. Mary's College of Minnesota, and in 1970, he received a Ph.D. from Caltech, where his adviser was Aron Kuppermann. In 1969, he joined the Chemistry faculty of the University of Minnesota, where he was promoted to Professor in 1976 and where he is currently Institute of Technology Distinguished Professor. He married his wife Jane in 1965, and they have two children, Sara and Stephanie.

* To whom correspondence should be addressed. E-mail: truhlar@umn.edu.

10.1021/ar040206v CCC: $33.50
Published on Web 08/17/2005

surface, and the nuclear motion on one surface, E_α, is coupled to that of another surface, E_β, by the nuclear momentum, which corresponds quantum mechanically to the action of the nuclear gradient operator on the electronic wave function. The dominant coupling in this representation is called the nonadiabatic coupling vector, $\mathbf{d}_{\alpha\beta}$.

Sometimes it is convenient to use wave functions that do not diagonalize the electronic Hamiltonian, for example, valence bond wave functions that correspond to a single electronic configuration. A familiar example is a curve crossing where the ground adiabatic state switches from ionic to covalent. Since valence bond states do not change suddenly when the nuclear geometry changes, $\mathbf{d}_{\alpha\beta}$ is often negligible in a valence bond representation;[19] the valence bond states are mainly coupled by the scalar electronic Hamiltonian (e.g., by the electronic Coulomb operator) rather than by the vector nuclear gradient. Unfortunately a quantitative description of a chemical system requires many more valence bond states than adiabatic states. However we define a valence-bond-like basis, called a "diabatic" basis, by a unitary transformation of the adiabatic electronic basis functions such that the vector couplings are small enough to neglect.[14,18−24] In the diabatic representation, the surfaces and their couplings may be written as a potential energy matrix, where the elements $U_{\alpha\alpha}$ are the surfaces, and $U_{\alpha\beta}$ are the diabatic couplings.

Some strengths of the adiabatic representation are that it is well defined, it is readily calculated using well-known electronic structure methods, and it often provides a good zero-order picture when the coupling is neglected. However, the coupling vectors are nonsmooth, even singular,[14,20−22] and inconvenient because of their high dimensionality. The diabatic picture, in contrast, inevitably neglects some coupling and is not unique, but it also has the important advantage that the couplings are smooth scalars.

Examples of the adiabatic and diabatic surfaces are shown in Figure 1, panels a and b, for ammonia. The diabatic surfaces and couplings, shown in Figure 1c, were obtained by the fourfold way[23] diabatization scheme. The first step in this systematic scheme for obtaining diabats from adiabats is to identify weak interaction regions of the potential energy surface that are defined as regions where the adiabatic states are well separated in energy, the nonadiabatic coupling is negligible, and adiabatic states are dominated by one or a small number of configuration state functions (CSFs) that are good prototypes for the diabatic states. The next step is to maximize a density functional involving three terms (called the threefold density criterion) that yields diabatic (i.e., smooth) molecular orbitals (DMOs) and to re-express the CSFs in terms of DMOs. In some strong interaction regions, the threefold criterion is insufficient to yield smoothly varying DMOs for the entire range of nuclear geometries, and one needs a reference orbital and a fourth criterion, resulting in the fourfold way.[23]

The results in Figure 1 were generated[25] using multiconfiguration quasidegenerate perturbation theory.[26] A

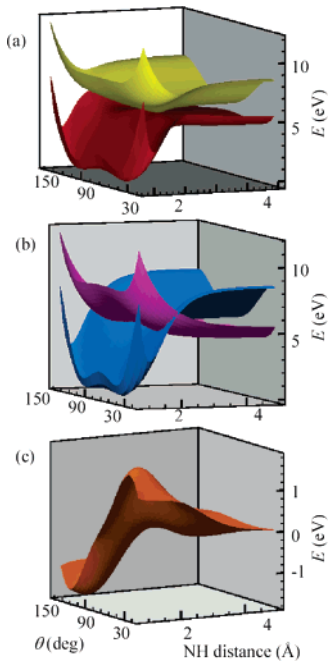

FIGURE 1. (a) Adiabatic and (b) diabatic potential energy surfaces for NH_3 as functions of one N−H bond distance and the inversion angle θ with the other coordinates fixed at their ground-state equilibrium values. The diabatic coupling is shown in panel c; it changes sign when one passes through a planar geometry. A conical intersection occurs in panel a at a planar geometry ($\theta = 90°$) at a N−H bond distance of 2.1 Å.

conical intersection occurs at planar geometries ($\theta = 90°$), which becomes an avoided crossing at other values of θ. Note that the diabatic surfaces are smooth functions of geometry and smoothly intersect with each other. The diabatic coupling is an odd function and changes sign about the D_{3h} planar geometry.

The adiabatic potential energy surfaces may be obtained by diagonalizing the diabatic potential energy matrix, and the nonadiabatic coupling may be obtained from the transformation so that either representation may be used for dynamics, even when the diabatic surfaces and couplings are computed directly.

3. Non-Born−Oppenheimer Trajectories

Next, we consider methods for incorporating non-BO coupling into classical trajectories. The nuclear motion is simulated by an ensemble (swarm) of independent trajectories, the initial conditions of which are distributed to mimic the distribution in position and momentum space of a quantum mechanical wave packet. Methods involving coupled trajectories (where the motion of each trajectory in the ensemble depends on the properties of other trajectories in the ensemble) are being developed,[27] but we do not consider them here.

As each trajectory in the ensemble evolves in time, the nuclear motion causes a change in the electronic state due to the breakdown of the BO approximation. This change results in a new effective potential energy felt by the trajectory. Non-BO trajectory methods must treat these effects accurately and self-consistently.

An electronic state reduced density matrix,[28] $\boldsymbol{\rho}$, is associated with each trajectory in the ensemble, where each diagonal element $\rho_{\alpha\alpha}$ is the probability of being in a given electronic state α, and $\rho_{\alpha\beta}$ are coherences (i.e., they correspond to the cross terms when the wave function is a coherent superposition of two states). The initial values of $\boldsymbol{\rho}$ are determined by the details of the problem, but typically a trajectory will start in a given state α such that $\rho_{\alpha\alpha} = 1$, and all other elements of $\boldsymbol{\rho}$ are initially zero. Equations for the time dependence of the elements of $\boldsymbol{\rho}$ along an arbitrary classical trajectory may be obtained using the Schrödinger equation and a semiclassical approximation, which yields[6,15]

$$i\hbar\dot{\rho}_{\alpha\alpha'} = \sum_{\gamma}(\rho_{\gamma\alpha'}F_{\gamma\alpha'} - \rho_{\alpha\gamma}F_{\alpha\gamma}) \tag{1}$$

where

$$F_{\alpha\alpha'} \equiv V_{\alpha\alpha'} - i\hbar\dot{\mathbf{R}}\cdot\mathbf{d}_{\alpha\alpha'} \tag{2}$$

$\dot{\mathbf{R}}$ is the classical nuclear velocity, $V_{\alpha\alpha} = E_\alpha$ and $V_{\alpha\beta} = 0$ for the adiabatic representation, and $V_{\alpha\alpha'} = U_{\alpha\alpha'}$ and $\mathbf{d}_{\alpha\alpha'} = 0$ for the diabatic representation. Adiabatically, $\mathbf{d}_{\alpha\beta}$ couples the states, and diabatically, $U_{\alpha\beta}$ couples them. When the coupling between states is zero, the diagonal elements of $\boldsymbol{\rho}$ do not change and there is no transfer of electronic state density. When coupling is nonzero, population transfer occurs ($\dot{\rho}_{\alpha\alpha} \neq 0$).

The nuclear coordinates **R** and momenta **P** evolve classically according to Newton's law

$$\dot{\mathbf{P}} = -\nabla V_{\text{eff}} \tag{3}$$

where V_{eff} is the effective semiclassical potential energy function that determines the non-BO trajectory.

An early[29] prescription for V_{eff}, motivated by the quantum Ehrenfest relations,[28] was to set the effective potential energy surface equal to a weighted average of the potential energy surfaces; this is equivalent to[2−4,30]

$$V_{\text{eff}} = \sum_{\alpha}\sum_{\alpha'}\rho_{\alpha\alpha'}V_{\alpha\alpha'} \tag{4}$$

We call this the semiclassical Ehrenfest (SE) method; it attempts to model the effective potential with an average. If the potential energies of the various electronic states are similar in topography and energy, then the nuclear motions in each state may be such that an SE trajectory is a reasonable approximation. For most chemical systems, however, this is not the case.[6,8] An important example of this is the case of weakly coupled surfaces; a SE trajectory will be dominated by the potential energy surface corresponding to the high-probability electronic state, and regions of space accessible only on the low-probability surface may not be properly explored. Furthermore, it is desirable to compute various properties of the products such as their internal energy, but it is not clear how to interpret the final state of a SE trajectory. For example an SE trajectory will finish a simulation in a mixed adiabatic electronic state (i.e., with more than one $\rho_{\alpha\alpha}$ nonzero), whereas the physics often requires that each trajectory ends with $\rho_{\alpha K} = \delta_{\alpha K}$ for some K (which may depend on the trajectory). The internal energies of mixed-state products are not reliable because they do not correspond to the internal energy distribution of a physically observable product. The SE method does have the desirable feature that it is formally independent of the choice of electronic representation.[2]

Next we consider semiclassical algorithms that go beyond the SE mean-potential approach.

3.1. Trajectory Surface Hopping. In trajectory surface-hopping methods, each trajectory, at any given time, is assigned an electronic state (the "occupied" electronic state K), and one assumes

$$V_{\text{eff}} = V_{KK} \tag{5}$$

The surfaces V_{KK} can be qualitatively different in the adiabatic and diabatic representations, and surface-hopping methods are often very sensitive to the choice of electronic representation. The single-surface propagation is interrupted by instantaneous transitions (called surface switches or hops) at which the occupied state is stochastically changed along the trajectory. The non-BO event is represented as a swarm of trajectories, each hopping between the various electronic states at different locations. When a hop occurs, the potential energy changes discontinuously, and the nuclear kinetic energy is adjusted to conserve total energy. Specifically, for an $\alpha \rightarrow \beta$ hop, the nuclear momentum is adjusted in the direction of $\mathbf{d}_{\alpha\beta}$. For some systems, surface-hopping methods may be inaccurate due to classically forbidden electronic transitions.[10] A surface hop is forbidden (or "frustrated") when the hopping algorithm calls for a hop to a higher-energy electronic state in regions where the nuclear momentum in the nonadiabatic coupling direction is insufficient to allow for an energy adjustment that will conserve total energy. When a frustrated hop is encountered, the self-consistency of the fraction of trajectories on each surface and the average electronic state populations is not maintained.

Several surface-hopping methods have been developed, which differ in their prescription for the hopping probability. In the Parlant−Gislason (PG) approach,[5] surface hopping is allowed at local maxima in the magnitude of a nonadiabatic coupling parameter Ω, and the hopping probability is determined nonlocally by the evolution of $\boldsymbol{\rho}$ between local minima of Ω. In the fewest-switches (FS) method of Tully,[6] the hopping probability is defined such that hopping is minimized and only occurs when there is a net flow (in an ensemble-averaged sense) of electronic state probability density out of the currently occupied state and such that the fraction of trajectories in each electronic state equals (in the absence of frustrated hops) the ensemble-averaged electronic state populations, $\rho_{\alpha\alpha}$. In the PG and FS methods, frustrated hops are ignored, and when a frustrated hop occurs, the trajectory does not change electronic states, which may cause significant errors in the predicted nonadiabatic probabilities.[10] The fewest switches with time uncertainty (FSTU) method[12] was developed to more accurately treat frustrated hops.

If a frustrated hop is encountered at time t_0, the system is allowed to hop at another time t_h along the trajectory, where, inspired by the time−energy uncertainty relations, t_h is small enough that

$$|t_0 - t_h|\Delta E \leq \hbar/2 \tag{6}$$

where ΔE is the amount of energy that the system would have to "borrow" to hop at time t_0. The resulting nonlocal hops may be thought of as including either uncertainty in the hopping times or tunneling into classically forbidden regions. If a suitable t_h cannot be found that meets the above criteria, then the frustrated hopping attempt is treated according to the "∇V prescription".[13]

3.2. Decay of Mixing Methods. Decay of mixing (DM) methods[9,17,31] are motivated by the recognition that when classical mechanics is used for the nuclear motion and quantum mechanics is used for the electronic motion (as is the case for all the methods considered here), the classical motion acts as a bath that relaxes the reduced electronic density matrix $\boldsymbol{\rho}$.[32] Several DM methods have been developed, and in this Account, we consider only the most theoretically justifiable of them, which is the coherent switches with decay of mixing (CSDM) method.[17,31] In the CSDM method, we calculate a relaxed density matrix by adding decay-of-mixing terms, $\dot{\rho}^{\mathrm{D}}_{\alpha\alpha'}$, to those in eq 1 such that time dependence of the relaxed density matrix, $\tilde{\boldsymbol{\rho}}$, is

$$\dot{\rho}_{\alpha\alpha'} = \dot{\rho}_{\alpha\alpha'} + \dot{\rho}^{\mathrm{D}}_{\alpha\alpha'} \tag{7}$$

where $\dot{\rho}_{\alpha\alpha'}$ is the fully coherent contribution given by eq 1. The DM terms are formulated such that the system decays to some pure state called the decoherent state or pointer state (labeled K throughout this section) according to some set of first-order decay times, $\tau_{\alpha K}$. The additional terms in eq 7 result in a decoherent force on the nuclear motion, and this force is directed along the decoherent direction $\hat{\mathbf{s}}$, which we take to be along the nonadiabatic coupling vector in strong interaction regions and along the vibrational momentum elsewhere. The pointer state is switched stochastically throughout the trajectory using equations similar to those used to switch the occupied state in the FS surface-hopping method. The relaxed density matrix $\tilde{\boldsymbol{\rho}}$, satisfying eq 7, is used to calculate V_{eff}, but the switching probability for the pointer state is governed by the coherent $\boldsymbol{\rho}$, satisfying eq 1, in each strong coupling region. A strong coupling region is the region between local minima in the surface coupling strength. This feature is similar to one aspect of the PG surface-hopping method discussed above and may be motivated by general arguments.[33] At a local minimum of the coupling strength, the switch-controlling coherent density matrix is synched to the relaxing one that controls the effective potential. This key element of the method differs from all previous surface-hopping and decay of mixing algorithms; as a result the amount of decoherence introduced between local minima of the coupling function depends on the length of the strong coupling region and the relaxation rates controlled by the $\tau_{\alpha\beta}$.

We emphasize that the DM potential energy surface switches gradually and smoothly between the various electronic surfaces; no hops are invoked, and therefore, no frustrated hops arise. In the DM formalism, we preserve SE-like motion in strong interaction regions or when the decay times are long.

Wave packet analyses have been carried out to elucidate the decay time.[34−36] In these analyses, one can identify pure dephasing arising from ensemble averaging over the phases associated with various trajectories and decoherence associated with divergence of nuclear wave packets associated with the various electronic states. Rossky and co-workers[35] have developed expressions for the decay time arising from the latter by considering minimum-uncertainty packets and by making semiclassical approximations. They obtain second-order decay as the leading term and extract a first-order rate constant from their analysis. A similar analysis[36] with less restrictive approximations gives first-order decay and a different, complicated form for the decay time. In both formulations, decay arises from the differences in forces and momenta on each pair of surfaces. The nuclear wave packets on the different surfaces have different momenta and experience different forces and get out of register. The off-diagonal elements (coherences) of the reduced electronic density therefore tend to zero when averaged over the nuclear wave packets. A systematic comparison of the various prescriptions for the decay time is not available. We have obtained good results using a simple expression that includes two key elements. In particular, at any instant along an CSDM trajectory, the system is decohering from each state α toward a single state K at a rate $\sim 1/\tau_{\alpha K}$, where we assume

$$\tau_{\alpha K} = \frac{\hbar}{|V_{\alpha\alpha} - V_{KK}|}\left(1 + \frac{E_0}{(\mathbf{P}\cdot\hat{\mathbf{s}})^2/2\mu}\right) \tag{8}$$

and E_0 is a parameter. We have found that setting E_0 equal to 0.1 hartree gives good results for several systems. The first factor may be identified as a pure dephasing term by noting that the phase factors associated with the off-diagonal elements of $\boldsymbol{\rho}$ spin in the complex plane on a time scale of $\hbar/|V_{\alpha\alpha} - V_{KK}|$. The factor in parentheses is required to turn off decoherence when the kinetic energy associated with the decoherent direction becomes small. Equation 8 is used in the CSDM calculations summarized in section 4.

4. Numerical Tests

As described above, several prescriptions for non-BO trajectories have been developed, and because semiclassical analyses and derivations necessarily contain ad hoc elements, validation of the proposed methods is required. Validation is often performed using simple one-dimensional models designed to represent prototypical electronically nonadiabatic interactions. One must be careful, however, when interpreting results from one-dimensional calculations, because one-dimensional systems may be very different from multidimensional systems.

We have developed several six-dimensional (after removing center-of-mass motion) systems[10,37,38] with which to test and validate the various non-BO trajectory methods. The systems are atom–diatom reactions

$$A^* + BC(v,j) \rightarrow \begin{cases} AB + C(E'_{int}) & (9a) \\ A + BC(E''_{int}) & (9b) \end{cases}$$

where the asterisk denotes an electronically excited A atom, and the BC diatom is initially in a specific rovibrational state (v,j). During the collision, the system de-excites either by reacting to form the products AB + C or nonreactively to form electronically quenched A + BC, where E'_{int} and E''_{int} are the final internal (i.e., rovibrational) energies of the AB and BC diatoms, respectively. There is no electronic angular momentum, and for all of the cases considered here, the total angular momentum of the system is zero. We consider six observables for each system: the probability P_R of reactive de-excitation (eq 9a); the probability P_Q of quenching (eq 9b); the total probability P_N of a nonadiabatic event, which is the sum of P_R and P_Q; the reactive branching fraction F_R, which is defined as P_R/P_N; the average internal energy of the diatomic fragment in eq 9a; and the average internal energy of the diatomic fragment in eq 9b.

We include three qualitatively different types of surfaces labeled avoided crossing (AC),[37] conical intersection (CI),[38] and weak interaction (WI),[10] each of which features a prototypical kind of nonadiabatic interaction, as illustrated for a typical member of each family in Figure 2. Within each family, we consider several coupling surfaces and various scattering conditions, as described elsewhere.[31] By averaging over several cases, we obtain a more robust measure of the accuracy of the non-BO trajectory methods.

Fully converged, fully six-dimensional quantum mechanical results were obtained[10,37,38] for each system in the test set using the outgoing wave variational principle.[39] To minimize the effect of quantal oscillations in the AC case when testing the approximate methods, we averaged over energy.

One can express potential energies and their couplings in either the adiabatic or diabatic representations, and dynamics carried out in these two representations are equivalent if no approximations are made. The SE method is formally independent of the choice of electronic representation, but the other methods do not preserve representation independence, and one must choose a representation to use for a given application. We will therefore test the non-BO trajectory methods using both the adiabatic and diabatic representations. For some simple cases, the choice of the preferred representation is straightforward. For example, for systems with large energy gaps, the adiabatic is expected to be preferred. However, for many non-BO problems it may not be possible to assign a single preferred electronic representation. For example, a system may have two or more distinct dynamical regions that differ in their preferred representation. Therefore, it is desirable to develop semiclassical methods that are accurate in both the diabatic and adiabatic electronic representations.

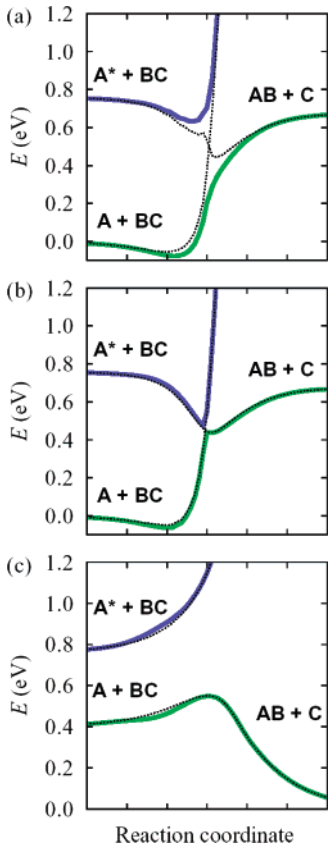

FIGURE 2. The ground-state adiabatic (green solid line), excited adiabatic (blue solid line), and diabatic (dotted lines) potential energies along the reaction coordinate for representative systems from the (a) AC, (b) CI, and (c) WI families of potential energy surfaces.

We first illustrate differences in the SE, CSDM, and surface-hopping approaches by considering a representative trajectory. Figure 3 shows the adiabatic and effective potential energies along an adiabatic trajectory for one of the CI systems for a typical set of initial coordinates and momenta. The CSDM pointer state switches between the upper and lower surfaces five times (at 591, 605, 611, 617, and 621 fs), and the trajectory leaves the strong interaction region reactively in a pure electronic state. The dynamics of the SE trajectory is similar to the dynamics of the CSDM trajectory until ~607 fs, where the mixed effective potential of the SE trajectory pushes the system away from the reactive molecular arrangement. The SE trajectory finishes the simulation nonreactively and with an effective potential energy that is a mixture of the upper and lower potential energy surfaces. The FSTU trajectory hops from the upper to the lower surface near the location of the first surface switch of the CSDM trajectory (at 591 fs) and proceeds reactively on the lower surface with qualitatively different dynamics than the CSDM and SE trajectories.

Five non-BO trajectory methods (SE, PG, FS, FSTU, and CSDM) have been tested against accurate quantum mechanical calculations using the AC, CI, and WI atom–diatom scattering test cases described above. Unsigned

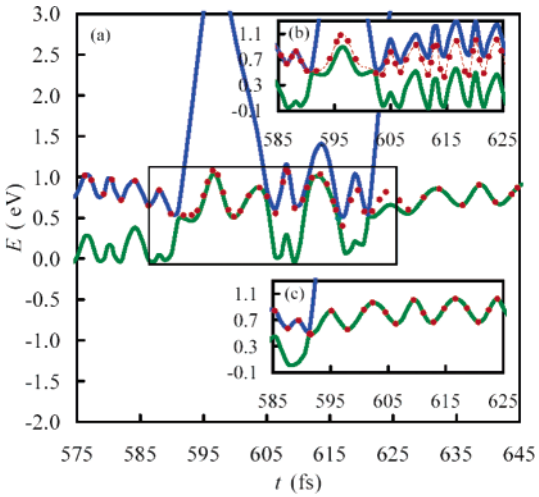

FIGURE 3. A representative trajectory for one of the CI systems in the adiabatic representation using the (a) CSDM, (b) SE, and (c) FSTU methods. For each method, the ground-state potential energy surface (green), the excited potential energy surface (blue), and the effective potential (red) are shown as a function of time. The interesting region (585−625 fs) is shown in a rectangular box for all methods.

Table 1. Average Unsigned Percentage Errors for Five Non-BO Trajectory Methods

method	rep[a]	AC[b]	CI[c]	WI[d]	overall[e]
		Mean Field			
SE	A/D	65	55	*f*	*f*
		Surface Hopping			
PG	A	97	49	201	116
	D	117	55	495	222
FS	A	64	48	29	47
	D	51	40	361	151
FSTU	A	52	52	24	43
	D	28	36	125	63
		Decay of Mixing			
CSDM	A	24	34	17	25
	D	19	28	32	26

[a] Electronic representation: adiabatic (A) or diabatic (D). [b] Averaged over nine cases. [c] Averaged over five cases. [d] Averaged over three cases. [e] Averaged over AC, CI, and WI, weighted equally. [f] These mean errors cannot be computed because the SE method incorrectly predicts no reactive trajectories for two WI cases.

percentage errors were averaged over each of the six observables and over the various test cases in each family of surfaces to provide a measure of the overall accuracy. The results[31] are summarized in Table 1.

It is difficult to isolate precisely what part of these errors arises from the treatment of the nonadiabatic event and how error much arises from the approximations involved even in single-surface trajectory simulations (such as the neglect of tunneling and quantized vibrations). One typically expects an error of ∼20−25% for a single-surface classical simulation in the gas phase. The error for the SE method of ∼60% for the AC and CI systems is therefore an indication that the SE method is not accurately modeling the nonadiabatic dynamics for these systems. Furthermore, for some of the WI systems (which feature low-probability events), the SE method is qualitatively incorrect. These problems outweigh the representation independence of the SE method and make the SE method unsuitable for practical work. The results for the surface-hopping methods show that the PG and FS methods are more representation-dependent and less accurate than the FSTU method, especially for the WI system where frustrated hopping is important. The FSTU method is also more accurate than the mean-field SE method; however, the errors are still greater than the typical error associated with single-surface classical dynamics, and sometimes the "wrong" choice of electronic representation can lead to significant errors. The CSDM method, however, features low representation dependence, as illustrated in Figure 4, where a trajectory with the same set of initial conditions is computed using the adiabatic and diabatic representations. Table 1 shows that the CSDM method has small errors for all three types of systems, indicating that it is a robust method of broad applicability.

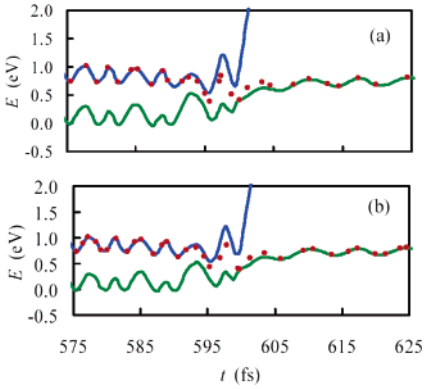

FIGURE 4. A representative pair of CSDM trajectories for the AC system in (a) adiabatic and (b) diabatic representations. In both representations the effective potential (red) coherently switches from the excited- (blue) to the ground-state (green) potential energy surfaces over an interval of ∼13 fs.

5. Conclusions

We discussed recent progress in extending molecular dynamics simulations to systems with electronically nonadiabatic transitions. These advances include the demonstration of a practical algorithm for the direct calculation of diabatic energies and couplings. The concept of a non-Born−Oppenheimer (non-BO) trajectory was discussed as a generalization of the usual single-surface molecular dynamics trajectory. Several non-BO methods, including surface-hopping and decay of mixing methods, were tested against accurate quantum mechanical results for 17 cases involving 10 representative model systems. The coherent switches with decay of mixing (CSDM) method, which is the result of a series of systematic improvements to the non-BO trajectory approach, is the most accurate of the non-BO methods tested. The overall error for this method is ∼25%, which is about the same as the error associated with single-surface classical trajectory methods. The CSDM method should be useful for qualitative and semiquantitative modeling of non-BO systems, just as molecular dynamics simulations have been used to study single-surface reactions in the past.

This work is supported in part by the National Science Foundation through Grant No. CHE03-49122.

References

(1) (a) Bunker, D. L. Classical trajectory methods. *Methods Comput. Phys.* **1971**, *10*, 287−325. (b) Truhlar, D. G.; Muckerman, J. T. Reactive scattering cross sections. III. Quasiclassical and semiclassical methods. In *Atom-Molecule Collision Theory: A Guide for the Experimentalist*; Bernstein, R. B., Ed.; Plenum: New York, 1979; pp 505−566. (c) Allen, M. P.; Tildesley, D. J. *Computer Simulation of Liquids*; Clarendon Press: Oxford, U.K., 1987. (d) Brooks, C. L., III; Karplus, M.; Pettitt, B. M. Proteins: A Theoretical Perspective of Dynamics, Structure, and Thermodynamics. *Adv. Chem. Phys.* **1988**, *71*, 1−259. (e) Benjamin, I. Molecular dynamics methods for studying liquid interfacial phenomena. In *Modern Methods for Multidimensional Dynamics Computations in Chemistry*; Thompson, D. L., Ed.; World Scientific: Singapore, 1998; pp 101−142. (f) Stanton, R. V.; Miller, J. L.; Kollman, P. A. Macromolecular dynamics. In *Modern Methods for Multidimensional Dynamics Computations in Chemistry*; Thompson, D. L., Ed.; World Scientific: Singapore, 1998; pp 355−383. (g) Rice, B. M. Molecular simulation of detonation. In *Modern Methods for Multidimensional Dynamics Computations in Chemistry*; Thompson, D. L., Ed.; World Scientific: Singapore, 1998; pp 472−528.

(2) Meyer, H.-D.; Miller, W. H. A classical analogue for electronic degrees of freedom in nonadiabatic collision processes. *J. Chem. Phys.* **1979**, *70*, 3214−3223.

(3) Micha, D. A. A self-consistent eikonal treatment of electronic transitions in molecular collisions. *J. Chem. Phys.* **1983**, *78*, 7138−7145.

(4) Amarouche, M.; Gadea, F. X.; Durup, J. A proposal for the theoretical treatment of multielectronic-state molecular dynamics: hemiquantal dynamics with the whole DIM basis (HWD). A test on the evolution of excited argon trimer(1+) cluster ions. *Chem. Phys.* **1989**, *130*, 145−157.

(5) Parlant, G.; Gislason, E. A. An exact trajectory surface hopping procedure: comparison with exact quantal calculations. *J. Chem. Phys.* **1989**, *91*, 4416−4418.

(6) (a) Tully, J. C. Molecular dynamics with electronic transitions. *J. Chem. Phys.* **1990**, *93*, 1061−1071. (b) Tully, J. C. Nonadiabatic dynamics. In *Modern Methods for Multidimensional Dynamics Computations in Chemistry*; Thompson, D. L., Ed.; World Scientific: Singapore, 1998; pp 34−72.

(7) Chapman, S. The classical trajectory-surface hopping approach to charge-transfer processes. *Adv. Chem. Phys.* **1992**, *82*, 423−483.

(8) Hack, M. D.; Truhlar, D. G. Nonadiabatic trajectories at an exhibition. *J. Phys. Chem. A* **2000**, *104*, 7917−7926.

(9) Hack, M. D.; Truhlar, D. G. A natural decay of mixing algorithm for non-Born−Oppenheimer trajectories. *J. Chem. Phys.* **2001**, *114*, 9305−9314.

(10) Jasper, A. W.; Hack, M. D.; Truhlar, D. G. The treatment of classically forbidden electronic transitions in semiclassical trajectory surface hopping calculations. *J. Chem. Phys.* **2001**, *115*, 1804−1816.

(11) Worth, G. A.; Robb, M. A. Applying direct molecular dynamics to nonadiabatic systems. *Adv. Chem. Phys.* **2002**, *124*, 355−431.

(12) Jasper, A. W.; Stechmann, S. N.; Truhlar, D. G. Fewest-switches with time uncertainty: a modified trajectory surface-hopping algorithm with better accuracy for classically forbidden electronic transitions. *J. Chem. Phys.* **2002**, *116*, 5424−5431; **2002**, *117*, 10427(E).

(13) Jasper, A. W.; Truhlar, D. G. Improved treatment of momentum at classically forbidden electronic transitions in trajectory surface hopping calculations. *Chem. Phys. Lett.* **2003**, *369*, 60−67.

(14) Jasper, A. W.; Kendrick, B. K.; Mead, C. A.; Truhlar, D. G. Non-Born−Oppenheimer chemistry: potential surfaces, couplings, and dynamics. *Adv. Ser. Phys. Chem.* **2004**, *14*, 329−391.

(15) Jasper, A. W.; Zhu, C.; Nangia, S.; Truhlar, D. G. Introductory lecture: Nonadiabatic effects in chemical dynamics. *Faraday Discuss.* **2004**, *127*, 1−22.

(16) Zhu, C.; Jasper, A. W.; Truhlar, D. G. Non-Born−Oppenheimer trajectories with self-consistent decay of mixing. *J. Chem. Phys.* **2004**, *120*, 5543−5557.

(17) Zhu, C.; Nangia, S.; Jasper, A. W.; Truhlar, D. G. Coherent switching with decay of mixing: an improved treatment of electronic coherence for non-Born−Oppenheimer trajectories. *J. Chem. Phys.* **2004**, *121*, 7658−7670.

(18) (a) Smith, F. T. Diabatic and adiabatic representations for atomic collision problems. *Phys. Rev.* **1969**, *179*, 111−123. (b) Mead, C. A.; Truhlar, D. G. Conditions for the definition of a strictly diabatic electronic basis for molecular systems. *J. Chem. Phys.* **1982**, *77*, 6090−6098. (c) Cimaraglia, R.; Malrieu, J.-P.; Persico, M.; Spiegelman, F. Quasi-diabatic states and dynamical couplings from ab initio CI calculations: A new proposal. *J. Phys. B* **1985**, *18*, 3073−3084.

(19) (a) Truhlar, D. G.; Duff. J. W.; Blais, N. C.; Tully, J. C.; Garrett, B. C. The quenching of Na(3 ^2P) by H_2: Interactions and dynamics. *J. Chem. Phys.* **1982**, *77*, 764−776. (b) Sidis, V. Diabatic potential energy surfaces for charge-transfer processes. *Adv. Chem. Phys.* **1992**, *82*, 73−134.

(20) Thompson, T. C.; Truhlar, D. G.; Mead, C. A. On the form of the adiabatic and diabatic representation and the validity of the adiabatic approximation for X_3 Jahn−Teller systems. *J. Chem. Phys.* **1985**, *82*, 2392−2407.

(21) Atchity, G. J.; Reudenberg. K. Determination of diabatic states through enforcement of configurational uniformity. *Theor. Chem. Acc.* **1997**, *97*, 47−58.

(22) Kupperman, A.; Abrol, R. Quantum reaction dynamics for multiple electronic states. *Adv. Chem. Phys.* **2002**, *124*, 283−322.

(23) (a) Nakamura, H.; Truhlar, D. G. The direct calculation of diabatic states based on configuration uniformity. *J Chem. Phys.* **2001**, *115*, 10353−10372. (b) Nakamura, H.; Truhlar, D. G. Direct diabatization of electronic states by the fourfold way. II. Dynamical correlation and rearrangement processes. *J Chem. Phys.* **2002**, *117*, 5576−5593. (c) Nakamura, H.; Truhlar, D. G. Extension of the fourfold way for the calculation of global diabatic potential energy surfaces of complex, multiarrangement, non-Born−Oppenheimer systems: Application to HNCO(S_0, S_1). *J Chem. Phys.* **2003**, *118*, 6618−6829.

(24) (a) Cederbaum, L. S. Born−Oppenheimer approximation and beyond. *Adv. Ser. Phys. Chem.* **2004**, *15*, 3−40. (b) Köppel, H. Diabatic representations: methods for the construction of diabatic electronic states. *Adv. Ser. Phys. Chem.* **2004**, *15*, 175−204.

(25) Nangia, S.; Truhlar, D. G. Direct calculation of coupled diabatic potential energy surfaces for ammonia. Manuscript in preparation.

(26) Nakano, H. Quasidegenerate perturbation theory with multiconfigurational self-consistent-field reference functions. *J Chem. Phys.* **2003**, *118*, 6618−6829.

(27) (a) Hack, M. D.; Wensmann, A. M.; Truhlar, D. G.; Ben-Nun, M.; Martínez, T. J. Comparison of full multiple spawning, trajectory surface hopping, and converged quantum mechanics for electronically nonadiabatic dynamics. *J. Chem. Phys.* **2001**, *115*, 1172−1186. (b) Ben-Nun, M.; Martinez, T. J. Ab initio quantum molecular dynamics. *Adv. Chem. Phys.* **2002**, *121*, 439−512. (c) Donoso, A.; Zheng, Y.; Martens, C. C. Simulation of quantum processes using entangled trajectory molecular dynamics. *J. Chem. Phys.* **2003**, *119*, 5010−5020.

(28) (a) Schiff, L. I. *Quantum Mechanics*, 3rd ed.; McGraw-Hill: New York, 1968. (b) Sakurai, J. J. *Modern Quantum Mechanics*; Addison-Wesley: Redwood City, CA, 1985.

(29) Mott, N. F. On the theory of excitation by collision with heavy particles. *Proc. Cambridge Philos. Soc.* **1931**, *27*, 553−560.

(30) Garcia-Vela, A.; Gerber, R. B.; Imre, D. G. Mixed quantum wave packet/classical-trajectory treatment of the photodissociation process argon hydrochloride (ArHCl) → argon + atomic hydrogen + atomic chlorine. *J. Chem. Phys.* **1992**, *97*, 7242−7250.

(31) Zhu, C.; Jasper, A. W.; Truhlar, D. G. Non-Born−Oppenheimer Liouville-von Neumann dynamics. Evolution of a subsystem controlled by linear and population-driven decay of mixing with decoherent and coherent switching. *J. Chem. Theory Comput.* **2005**, *1*, 527−540.

(32) (a) Bittner, E. R.; Rossky, P. J. Quantum decoherence in mixed quantum-classical systems: nonadiabatic processes. *J. Chem. Phys.* **1995**, *103*, 8130−8143. (b) Prezhdo, O. V.; Rossky, P. J. Evaluation of quantum transition rates from quantum-classical molecular dynamics simulations. *J. Chem. Phys.* **1997**, *107*, 5863−5878. (c) Wong, K. F.; Rossky, P. J. Dissipative mixed quantum-classical simulation of the aqueous solvated electron system. *J. Chem. Phys.* **2002**, *116*, 8418−8428. Wong, K. F.; Rossky, P. J. Solvent-induced electronic decoherence: Configuration dependent dissipative evolution for solvated electron systems. *J. Chem. Phys.* **2002**, *116*, 8429−8438.

(33) Thachuk, M.; Ivanov, M. Y.; Wardlaw, D. M. A semiclassical approach to intense-field above-threshold dissociation in the long wavelength limit. II. Conservation principles and coherence in surface hopping. *J. Chem. Phys.* **1998**, *109*, 5747−5760.

(34) Fiete, G. A.; Heller, E. J. Semiclassical theory of coherence and decoherence. *Phys. Rev. A* **2003**, *68*, 22112/1−10.

(35) Turi, L.; Rossky, P. J. Critical evaluation of approximate quantum decoherence rates for an electronic transition in methanol solution. *J. Chem. Phys.* **2004**, *120*, 3688−3698.

(36) Jasper, A. W.; Truhlar, D. G., Electronic decoherence times for non-Born−Oppenheimer trajectories. *J. Chem. Phys.*, in press.

(37) Volobuev, Y. L.; Hack, M. D.; Topaler, M. S.; Truhlar, D. G. Continuous surface switching: an improved time-dependent self-consistent-field method for nonadiabatic dynamics. *J. Chem. Phys.* **2000**, *112*, 9716–9726.
(38) Jasper, A. W.; Truhlar, D. G. Conical intersections and semiclassical trajectories: comparison to accurate quantum dynamics and analyses of the trajectories. *J. Chem. Phys.* **2005**, *122*, 44101/1–16.
(39) See Tawa, G. J.; Mielke, S. L.; Truhlar, D. G.; Schwenke, D. W. Linear algebraic formulation of reactive scattering with general basis functions. In *Advances in Molecular Vibrations and Collisional Dynamics*; Bowman, J. M., Ed.; JAI: Greenwich, CT, 1994; Vol. 2B, pp 45–116 and references therein.

AR040206V